

# Simulation of Tropospheric Ozone with MOZART-2: An Evaluation Study over East Asia

LIU Qianxia<sup>\*1,3</sup> (刘茜霞), ZHANG Meigen<sup>2</sup> (张美根), and WANG Bin<sup>1</sup> (王 斌)

<sup>1</sup>*State Key Laboratory of Numerical Modeling for Atmospheric Sciences and Geophysical Fluid Dynamics (LASG),  
Institute of Atmospheric Physics, Chinese Academy of Sciences, Beijing 100029*

<sup>2</sup>*State Key Laboratory of Atmospheric Boundary Layer Physics and Atmospheric Chemistry (LAPC),  
Institute of Atmospheric Physics, Chinese Academy of Sciences, Beijing 100029*

<sup>3</sup>*Graduate School of the Chinese Academy of Sciences, Beijing 100049*

(Received 3 November 2004; revised 10 January 2005)

## ABSTRACT

Climate changes induced by human activities have attracted a great amount of attention. With this, a coupling system of an atmospheric chemistry model and a climate model is greatly needed in China for better understanding the interaction between atmospheric chemical components and the climate. As the first step to realize this coupling goal, the three-dimensional global atmospheric chemistry transport model MOZART-2 (the global Model of Ozone and Related Chemical Tracers, version 2) coupled with CAM2 (the Community Atmosphere Model, version 2) is set up and the model results are compared against observations obtained in East Asia in order to evaluate the model performance. Comparison of simulated ozone mixing ratios with ground level observations at Minamitorishima and Ryori and with ozonesonde data at Naha and Tateno in Japan shows that the observed ozone concentrations can be reproduced reasonably well at Minamitorishima but they tend to be slightly overestimated in winter and autumn while underestimated a little in summer at Ryori. The model also captures the general features of surface CO seasonal variations quite well, while it underestimates CO levels at both Minamitorishima and Ryori. The underestimation is primarily associated with the emission inventory adopted in this study. Compared with the ozonesonde data, the simulated vertical gradient and magnitude of ozone can be reasonably well simulated with a little overestimation in winter, especially in the upper troposphere. The model also generally captures the seasonal, latitudinal and altitudinal variations in ozone concentration. Analysis indicates that the underestimation of tropopause height in February contributes to the overestimation of winter ozone in the upper and middle troposphere at Tateno.

**Key words:** tropospheric ozone, global chemical transport model, MOZART-2, tropopause, East Asia

---

## 1. Introduction

Research on the interaction between ozone ( $O_3$ ) and climate is evolving rapidly, mainly because of the important influences of ozone on climate. On the one hand, ozone is an important radiative gas which has a positive radiative forcing on climate in the troposphere and a negative radiative forcing in the stratosphere, especially when tropospheric ozone and its precursors [carbon monoxide (CO), nitrogen oxides ( $NO_x$ ), non-methane hydrocarbons (NMHCs), etc.] are on the increase (IPCC, 2001); on the other hand, it is a key species that could ultimately determine the oxidiz-

ing capacity of the atmosphere and control chemical lifetimes of other atmospheric species. Some studies have showed that increased surface emissions of chemical compounds caused by industrial activities at mid-latitudes in the Northern Hemisphere and by biomass burning in the Tropics since the middle of the 19th century have produced an increase in the abundance of tropospheric ozone along with a reduction in the oxidizing capacity of the atmosphere (globally averaged OH concentration reduced by 17% and methane lifetime enhanced by 1.5 years; Brasseur et al., 1998a). Therefore, tropospheric ozone can indirectly influence

\*E-mail: lqx@mail.iap.ac.cn

concentrations of other greenhouse gases in the atmosphere, which then could decisively influence us to correctly estimate how variations in atmospheric chemical constituents affect climate changes. From this point of view, we urgently need to obtain a better understanding of the processes responsible for the global tropospheric ozone distributions. However, the very limited observations of ozone during the preindustrial period and the limited coverage of upper tropospheric ozone at present cannot satisfy the demand (Bernstein and Isaksen, 1997), so a three-dimensional global atmospheric chemistry model coupled with a global climate model can not only allow us to reasonably estimate distributions of ozone but also help us to correctly predict climate changes by human activities.

In China, few reports have been made on the interactions between ozone and climate. Liu et al. (2003; 2004) made several numerical tests to investigate the influences of pollutant emissions on the distributions of ozone and other related tracers in China by using a three-dimensional global chemistry transport model (OSLO CTM2; Bernstein and Isaksen, 1997). However, these studies did not discuss in detail the interactions between climate and chemical species.

In the past three years, Chinese scientists have been trying to develop a global climate system model, and a coupling system would include many components such as atmosphere, ocean, ocean-ice, land and atmospheric chemistry, etc. (cf. <http://www.lasg.ac.cn>). Incorporating chemical processes into the system is one of the most important objectives.

As the first step, we have successfully coupled the atmospheric chemistry model MOZART-2 (the global Model of Ozone and Related Chemical Tracers, version 2; Horowitz et al., 2003) with the global climate model CAM2 (the Community Atmosphere Model, version 2; Collins et al., 2002). In this paper, we focus on the evaluation of the model performance with observations from East Asia.

## 2. Model description

MOZART is built on the framework of the Model of Atmospheric Transport and Chemistry (MATCH; Rasch et al., 1997), which includes representations of advection, convective transport, boundary layer mixing, and dry and wet deposition. Advection of tracers is based on the flux-form semi-Lagrangian advection scheme (Lin and Rood, 1996), and convective flux transport is re-diagnosed using the Hack (1994) scheme for shallow and mid-level convection and the Zhang and McFarlane (1995) scheme for deep convection. Vertical diffusion within the boundary layer is represented using the parameterization of Holtslag and Boville (1993). A detailed description of MOZART-2 is given by Horowitz et al. (2003).

In this study, MOZART-2 is used to simulate global ozone distributions with meteorological fields from CAM2 instead of its original meteorological driver—MACCM3 (Middle Atmosphere Community Climate Model version 3; Kiehl et al., 1998). CAM2 has a horizontal resolution of approximately  $2.8^\circ \times 2.8^\circ$  and 26 hybrid vertical levels from the surface to 2.917 hPa. The precalculated meteorological fields include dynamical and physical variables for resolving advective transport, smaller-scale exchanges and wet scavenging, and are available every 3 hours. The timestep for chemical and transport integration in MOZART-2 is 20 min for each.

MOZART-2 considers surface emissions of chemical compounds such as  $\text{N}_2\text{O}$ ,  $\text{CH}_4$ , NMHCs,  $\text{CO}$ ,  $\text{NO}_x$ ,  $\text{HCHO}$ , and acetone. The chemical mechanism used in the model contains 63 chemical species and 168 reactions (including 33 photolysis reactions). Emissions from fossil fuel combustion, fuelwood burning, and agricultural waste burning are based on the Emission Database for Global Atmospheric Research (EDGAR) version 2.0 (Olivier et al., 1996), and biomass burning emissions from the Tropics and the Extratropics are adopted from Hao and Liu (1994) and Müller (1992), respectively. Biogenic emissions of hydrocarbons from vegetation are taken from the Global Emissions Inventory Activity (GEIA; Guenther et al., 1995) for isoprene and monoterpenes and from Müller (1992) for other species. Biogenic emissions of methane from rice paddies and ruminants are based on EDGAR (Olivier et al., 1996), while those from wetlands and termites are based on the work of Müller (1992). Emissions of  $\text{CO}$ , methane and NMHCs from the ocean are included in the model with distributions as in the work of Brasseur et al. (1998b). Lightning and aircraft emissions are also considered in this model; for more details, please see Horowitz et al. (2003).

Stratospheric concentrations of several long-lived species ( $\text{O}_3$ ,  $\text{NO}_x = \text{NO} + \text{NO}_2$ ,  $\text{HNO}_3$ ,  $\text{N}_2\text{O}_5$ , and  $\text{N}_2\text{O}$ ) are constrained by relaxation toward zonally- and monthly- averaged values from the middle atmosphere model Study of Transport and Chemical Reactions in the Stratosphere (STARS; Brasseur et al., 1997; for species other than  $\text{O}_3$ ) and from “observed” ozone climatologies from Logan (1999; for  $\text{O}_3$  below 100 hPa) and the Halogen Occultation Experiment (HALOE; Randel et al., 1998; for  $\text{O}_3$  above 100 hPa). This relaxation is performed from the local thermal tropopause (defined by a lapse rate of  $2 \text{ K km}^{-1}$ ) to the model top at each timestep, with a relaxation time constant of 10 days.

## 3. Results and discussions

### 3.1 Surface $\text{O}_3$ distributions

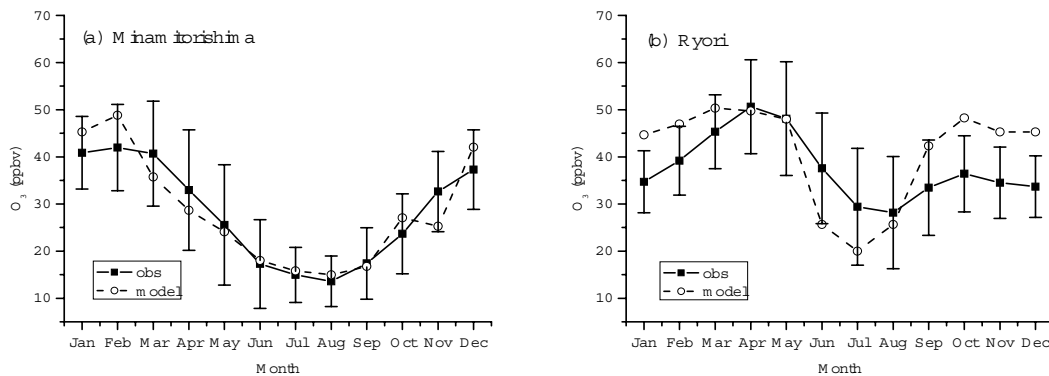
MOZART-2 is driven by meteorology from CAM2.

The meteorology is intended to simulate a “typical” year, not any specific year of observations. In order to compare model results with observations, we compare monthly mean model results with the corresponding multiyear mean observations (Logan, 1999). The observation data at Tateno and Naha are those from 1980 to 1995 and from 1989 to 1995, respectively. In this study, the observed surface  $O_3$  and CO mixing ratios at Minamitorishima and Ryori in Japan are obtained from the NOAA/Climate Monitoring and Diagnostics Laboratory (CMDL) flask measurement network (SASAKI, 2003), and their observation data are from 1994 to 2003 and from 1991 to 2002, respectively.

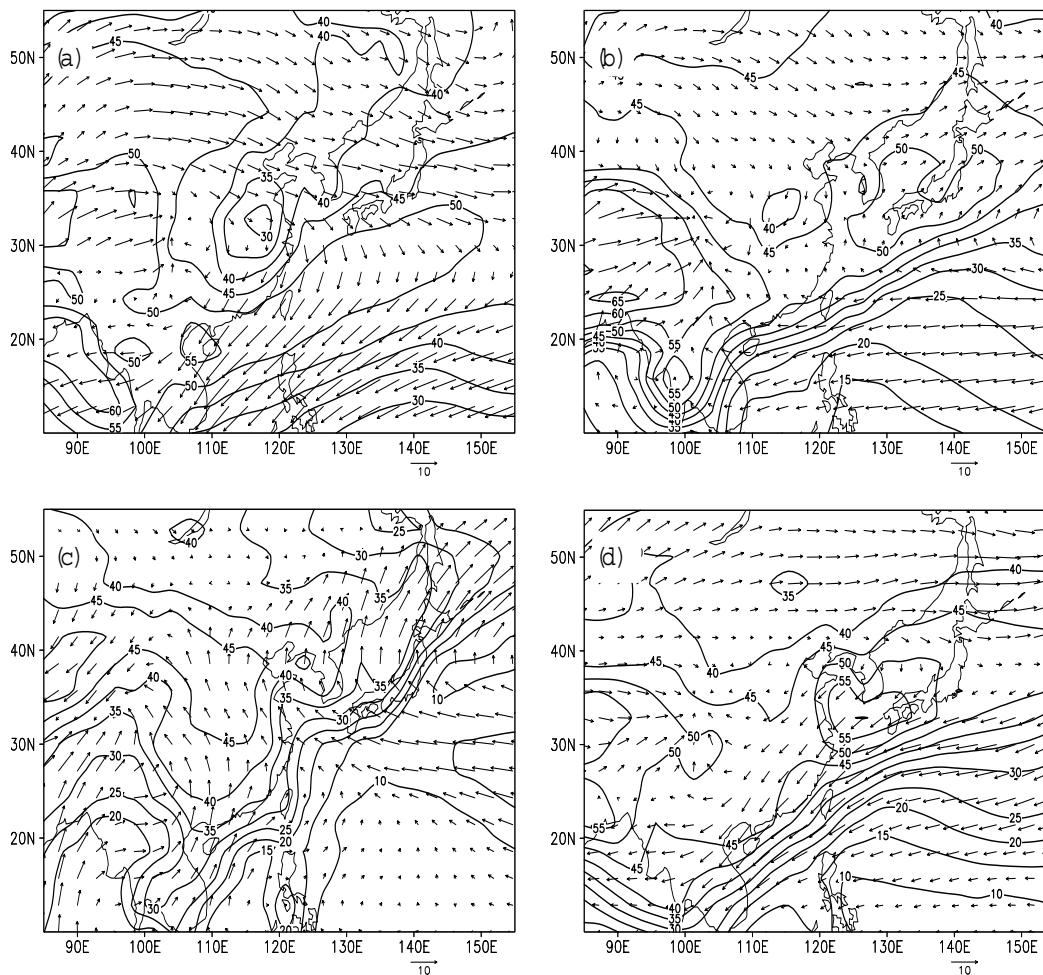
Minamitorishima, located about 2000 km south-east of Tokyo, is an isolated island. It has an area of about  $1.4 \text{ km}^2$  and a coastline about 5.5 km long in the Pacific. The sampling site is at  $24^\circ 18' \text{N}$ ,  $153^\circ 58' \text{E}$ , 8 m above sea level. The Ryori site is located halfway up a mountainous cape in central Japan facing the Pacific Ocean at  $39^\circ 02' \text{N}$ ,  $141^\circ 49' \text{E}$ , and 260 m above the sea level.

Figure 1 shows the seasonal variations of monthly mean surface ozone mixing ratios measured at Minamitorishima (Fig. 1a) and Ryori (Fig. 1b). Also shown are the model results at the lowest layer, approximately 30 m above the ground. At Minamitorishima, the observed seasonal ozone variation shows a summer minimum and a winter maximum, which is a typical pattern of many remote locations both in the Northern and Southern Hemispheres (Monks et al., 2000). The simulation can successfully capture this pattern with a little overestimation in winter and a slight underestimation in spring. By contrast, the observed surface ozone seasonal variation at Ryori exhibits a clear spring maximum characteristic of the

surface ozone seasonal cycles in a very clean and remote atmosphere across mid-latitudes in the Northern Hemisphere. From Fig. 1b, we can see that a spring ozone maximum in April can be simulated well compared with the observed value, however, the model slightly overestimates ozone concentrations in both winter and autumn and underestimates them a little in summer. The seasonal variation in ozone concentration depends on a multitude of factors, such as the proximity to large source areas of ozone precursors, geographical location and meteorological factors (Logan, 1985), so the above two different kinds of ozone seasonal cycle patterns may reflect two different kinds of ozone production modes. For example, Minamitorishima is surrounded by ocean and its location is south of  $30^\circ \text{N}$ , therefore on a seasonal basis its seasonal cycle pattern can be rationalized in terms of photochemistry determining the lower bound for ozone levels while entrainment from the free troposphere across an effective concentration gradient controls the upper bound (Monks et al., 2000). Good model results at this site show that the model can grasp the general features of ozone variations in a clean marine boundary layer. Ryori is located north of  $30^\circ \text{N}$ , belonging to the East Asia monsoon area, which can be greatly affected by continental outflow except in summer. As can be seen from Fig. 2c, in July the dominant wind flow is southeasterly, so the minimum should be ascribed to southeasterly flow of low ozone air from the tropical Pacific as part of the summer monsoon. On the other hand, the dominant flow in other seasons is found to be westerly from Figs. 2a, 2b and 2d, so the continental outflow should be prevailing, which brings more continental pollutants to the remote clean regions. Further analy-



**Fig. 1.** Seasonal variations of simulated monthly mean ozone mixing ratios (dashed lines, ppbv) at the lowest layer ( $\sim 30$  m above ground) and observed ground-level monthly mean ozone mixing ratios (solid lines, ppbv) at (a) Minamitorishima ( $24.30^\circ \text{N}$ ,  $153.97^\circ \text{E}$ ) over the period 1994–2003 and (b) Ryori ( $39.03^\circ \text{N}$ ,  $141.82^\circ \text{E}$ ) over the period 1991–2002. Error bars represent one standard deviation of the observed ground-level monthly mean ozone mixing ratios.



**Fig. 2.** Monthly average horizontal distributions of  $O_3$  mixing ratios (ppbv) and monthly wind fields (units:  $m\ s^{-1}$ ) at a height of about 30 m above ground in (a) January (b) April (c) July (d) October.

sis has been made regarding the stratospheric and photochemical contributions toward the spring maximum at Ryori. As a case in point, we focus on the ozone maximum in April. By calculation, it is found that two-thirds of the tropospheric ozone concentrations come from photochemical production and one-third from stratospheric origin, so we think that the spring ozone maximum at this site should be mainly ascribed to the photochemical origin. However, the overestimation of ozone in wintertime and autumn cannot simply be ascribed to more downward influx from stratospheric ozone, because surface ozone concentrations are little affected by stratospheric origin (Follows and Austin, 1992; Zhang et al., 2004), just as discussed above. The main reason could result from the failure to reveal the influences of monsoon climate on pollutant distributions. Further work will be done to investigate their inherent relationships.

Surface CO mixing ratios are also compared with

observations at Minamitorishima (Fig. 3a) and Ryori (Fig. 3b). From Fig. 3 we can see that the general features of mean simulated CO seasonal variations can be reproduced quite well in spite of some underestimations at both Minamitorishima (Fig. 3a) and Ryori (Fig. 3b). In this study, the observation data used for comparison are multi-year averages from the early 1990s to the early 2000s while the emissions are intended to be representative of those in the early 1990s, so the underestimations may be related to the adopted emission inventory. The model results, on the other hand, have also showed us the trend of increasing pollutant emissions by industrial development and population expansion over East Asia. Also, we can see a summer minimum and a winter-spring maximum in CO seasonal variations, and this phenomenon should be regarded as the result of photochemical reaction. Because the major sink of CO is its reaction with OH, and in summer the production of OH is higher than

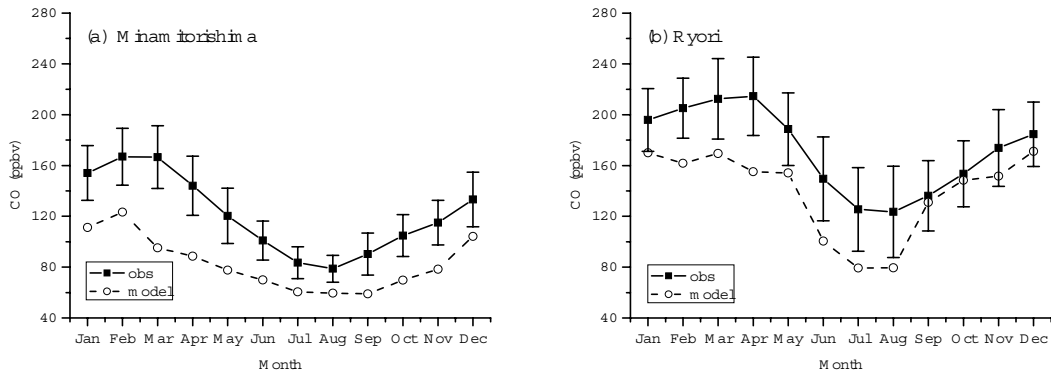


**Fig. 3.** As Fig. 1 but for simulated monthly mean CO mixing ratios (ppbv).

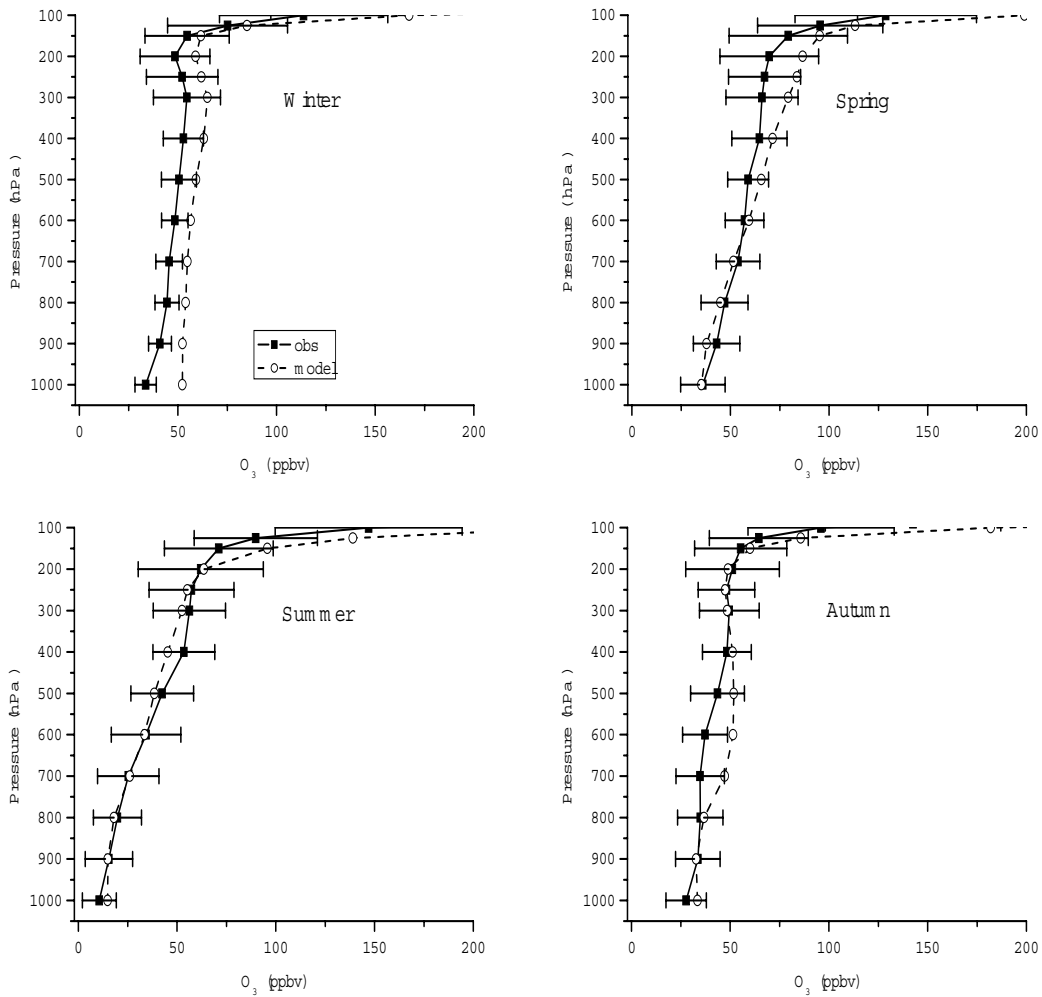


**Fig. 4.** Comparison of observed (solid lines) and simulated (dashed lines) seasonal vertical profiles of ozone volume mixing ratios (ppbv), and standard deviations of the observations (error bars). Observations are from ozonesonde measurements compiled by Logan (1999) at Naha (26°12'N, 127°41'E) in Japan.

in any other season, thus a CO minimum arises. However, in winter, inactive photochemical activities, a longer lifetime of CO and intense surface emissions could all contribute to the winter and subsequent spring maximum. The well-simulated effect of CO shows that the model can perfectly capture the key mechanism affecting distributions of CO.

### 3.2 O<sub>3</sub> vertical profiles

The model results compared with observations at Naha (26°12'N, 127°41'E) and Tateno (36°03'N, 140°08'E) are shown in Figs. 4 and 5. The observations are from multiple years of sonde measurements compiled by Logan (1999). These figures show that at both sites the vertical gradient and magnitude of ozone can be well simulated except that there is a little overestimation in winter. For example, summer ozone concentrations at Naha and spring ones at Tateno are in good agreement with observations. At Naha, there is a little

overestimation of spring upper-tropospheric ozone and autumn middle-tropospheric ozone. At Tateno, there are some underestimations below the tropopause in summer and a few overestimations between the mid troposphere and upper troposphere in autumn. Also, we can see that the simulated effect of ozone concentrations around the tropopause in different seasons varies greatly at both sites, and the biggest difference arises in winter. For example, an overestimation can be seen around the tropopause, and the deviation from the observation at Tateno seems a little bigger.

### 3.3 Seasonal variations

Time series of monthly mean ozone mixing ratios in the lower (800 hPa), middle (500 hPa) and upper (300 hPa) troposphere are compared with those derived from ozonesonde measurements over Japan (c.f. Fig. 6). In general, the model captures the seasonal,

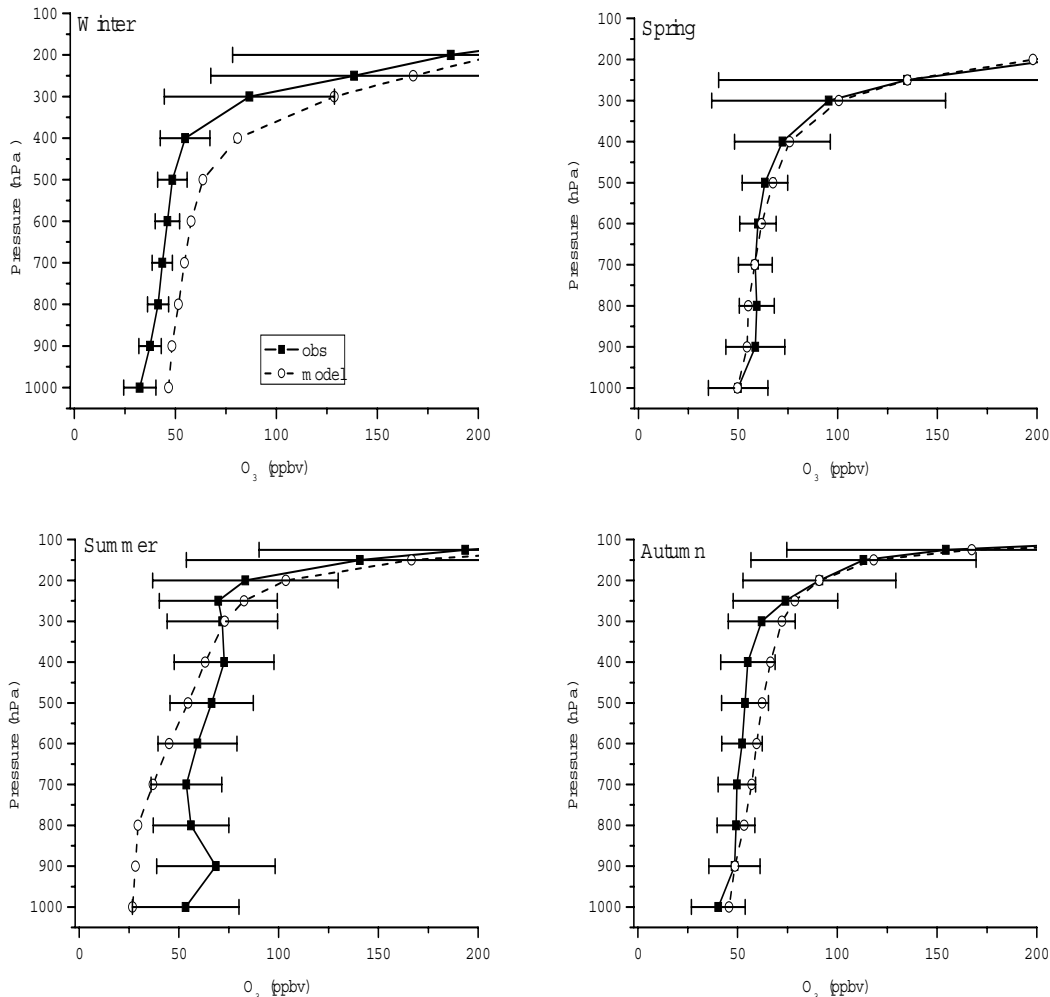
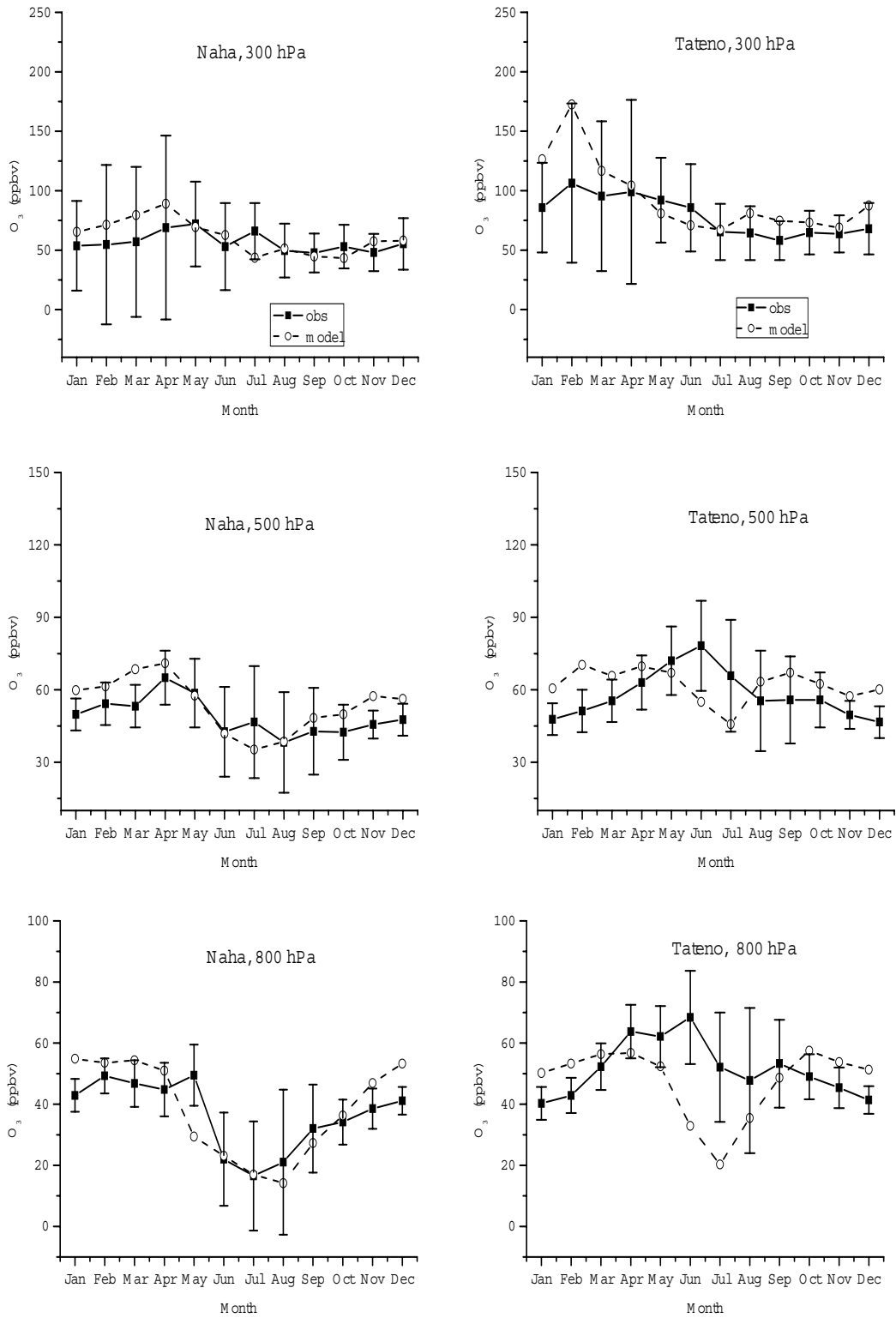
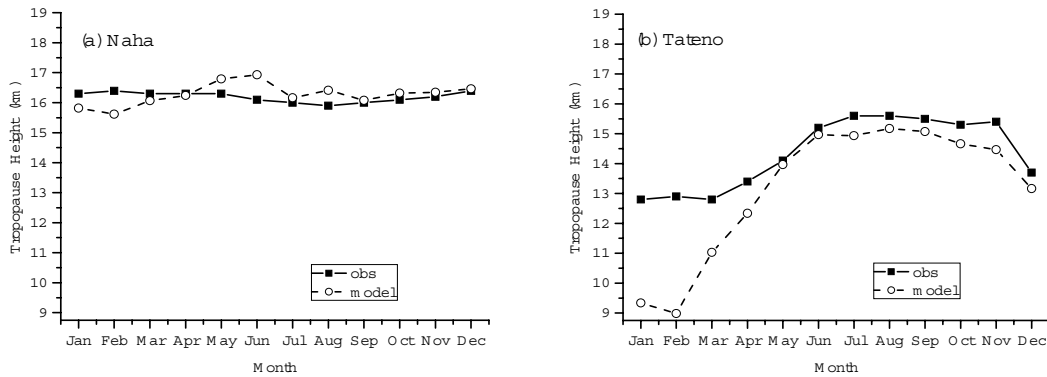


Fig. 5. As Fig. 4 but for Tateno (36°03'N, 140°08'E) in Japan.



**Fig. 6.** Time series of monthly mean ozone mixing ratios over the period 1980–1995 (1989–1995 for Naha) from ozonesonde measurements over Japan (Logan, 1999) (solid lines), against mean modeled mixing ratios (dashed lines). Error bars are defined as one standard deviation and reflect the variability during the month over the whole multiyear period.



**Fig. 7.** Comparison of the simulated (dashed lines) and the observed (solid lines) tropopause height (units: km) both at (a) Naha ( $26^{\circ}\text{N}$ ,  $128^{\circ}\text{E}$ ) and (b) Tateno ( $36^{\circ}\text{N}$ ,  $140^{\circ}\text{E}$ ).

latitudinal and altitudinal variations of ozone concentrations reasonably well, with mixing ratios mostly lying within one standard deviation of the measurements. There are some discrepancies in the lower troposphere, such as at Tateno where summer ozone formation from the nearby Tokyo area is not captured well, and where surface mixing ratios in winter tend to be overestimated. However, the variations in the altitude of the tropopause with season are reproduced well, and the latitudinal gradient of ozone variations in the upper troposphere are captured, though the gradient is less steep in winter as seen in the overestimation over Tateno. Also, from the observed curves, we can see that there is a summer maximum at Tateno ( $36^{\circ}\text{N}$ ) and a summer minimum at Naha ( $26^{\circ}\text{N}$ ) in the lower troposphere, while the corresponding maximum ozone concentration at Tateno is simulated in October, lagging behind the observed maximum by four months. However, at Naha, the summer minimum can be simulated quite well, and the minimum can be explained by southeasterly flow of low ozone air from the tropical Pacific as part of the summer monsoon (c.f. Fig. 2c), reflecting that the wind field in the model is reasonable.

In order to investigate some problems of the above overestimations in winter, comparisons between the simulated and the observed tropopause height at Naha and Tateno are examined.

Figure 7 shows a comparison of the simulated (dashed lines) and the observed (solid lines) tropopause height at Naha and Tateno. The observed is a mean statistical value (Maxobep, 1983). From the simulated curves, the underestimation of tropopause height before April is shown at both sites, and then in the coming months, a different overestimation appears, especially the peak that can be seen in June at Naha. Variations of the tropopause height can influence ozone concentrations around the tropopause, as can be seen from the simulated effect for ozone at 300 hPa at Tateno in winter; for example, the

higher simulated ozone level appearing in February at 300 hPa could be ascribed to the far lower simulated tropopause height. Furthermore, the influence can be spread to the mid troposphere, so the same phenomenon can also be seen at 500 hPa, however, ozone concentrations in the lower troposphere are little affected. Austin and Follows (1991) showed from a mean-mode analysis of the Payerne ozone record that at 300 hPa, 25% of the observed mixing ratio could be ascribed to cross-tropopause flux annually. An expanded zonal average model (Follows and Austin, 1992) demonstrates that ozone of stratospheric origin has a very small effect (5% at most) on surface ozone. Therefore, the key reason leading to the underestimation of ozone at 800 hPa in summer at Tateno seems to be a smaller connection with its corresponding tropopause height. Tateno is very close to Tokyo, so the anthropogenic influence would be prominent, especially in summer, when isolation, temperature and the abundant precursors are more favorable to ozone formation. However, failure to grasp the main features may be related to the coarse resolution of the model, for it would be very difficult to distinguish a clean site from a polluted one at such a coarse resolution.

#### 4. Summary

As the first step to realize the coupling goal of an atmospheric chemistry model and a climate model, a three-dimensional global atmospheric chemistry transport model MOZART-2 (the global Model of Ozone and Related Chemical Tracers, version 2) coupled with CAM2 (the Community Atmosphere Model, version 2) is set up and the model results are compared against observations obtained in East Asia in order to evaluate the model performance. The model-calculated mixing ratios of ozone and carbon monoxide are compared against surface observations at Minamitorishima and Ryori, and the vertical profiles and seasonal variations



of ozone are compared with multiyear ozonesonde data at Naha and Tateno. It is found that the model can reasonably reproduce two typical patterns of surface ozone seasonal variations, and that one shows a summer minimum and a winter maximum represented by Minamitorishima while the other shows a spring maximum represented by Ryori. The observed ozone concentrations can be reproduced reasonably well at Minamitorishima but tend to be slightly overestimated in winter and autumn, while they tend to be underestimated a little in summer at Ryori. The model can also capture the general features of surface CO seasonal variations, while it underestimates CO levels at both Minamitorishima and Ryori. The underestimation is primarily associated with the emission inventory adopted in this study.

Compared with the ozonesonde data at Naha and Tateno, the simulated vertical gradient and magnitude of ozone can be reasonably well simulated with a little overestimation in winter, especially in the upper troposphere. The model can also generally capture the seasonal, latitudinal and altitudinal variations in ozone concentrations.

Compared with the statistical observation values of tropopause height, the underestimation of tropopause height in February is found to contribute to the overestimation of winter ozone in the upper and middle troposphere at Tateno.

**Acknowledgments.** The authors wish to thank Dr. Stacy Walters at National Center for Atmospheric Research (NCAR) and Professor Brasseur G.P. at Max Planck Institute for Meteorology (MPI) for the MOZART-2 source code and for their valuable help. This work was partly supported by the Fund for Innovative Research Groups (Grant No. 40221503) and the National Natural Science Foundation of China (Grant No. 40233031).

## REFERENCES

- Austin, J. F., and M. J. Follows, 1991: The ozone record at Payerne: An assessment of the cross-tropopause flux. *Atmos. Environ.*, **25**, 1873–1880.
- Berntsen, T. K., and I. S. A. Isaksen, 1997: A global three-dimensional chemical transport model for the troposphere, 1. Model description and CO and ozone results. *J. Geophys. Res.*, **102**, 21239–21280.
- Brasseur, G. P., X. X. Tie, P. J. Rasch, and F. Lefevre, 1997: A three-dimensional simulation of the Antarctic ozone hole: Impact of anthropogenic chlorine on the lower stratosphere and upper troposphere. *J. Geophys. Res.*, **102**, 8909–8930.
- Brasseur, G. P., J. T. Kiehl, J.-F. Müller, T. Schneider, C. Granier, X. Tie, and D. Hauglustaine, 1998a: Past and future changes in global tropospheric ozone: Impact on radiative forcing. *Geophys. Res. Lett.*, **25**, 3807–3810.
- Brasseur, G. P., D. A. Hauglustaine, S. Walters, P. J. Rasch, J.-F. Müller, C. Granier, and X. X. Tie, 1998b: MOZART, a global chemical transport model for ozone and related chemical tracers: 1. Model description. *J. Geophys. Res.*, **103**, 28265–28289.
- Collins, W. D., and Coauthors, 2002: Description of the NCAR Community Atmosphere Model (CAM2). [Available from <http://www.cesm.ucar.edu/models/atm-cam/docs/description/>].
- Follows, M. J., and J. F. Austin, 1992: A zonal average model of the stratospheric contributions to the tropospheric ozone budget. *J. Geophys. Res.*, **97**, 18047–18060.
- Guenther, A. and Coauthors, 1995: A global model of natural volatile organic compound emissions. *J. Geophys. Res.*, **100**, 8873–8892.
- Hack, J. J., 1994: Parameterization of moist convection in the NCAR community climate model (CCM2). *J. Geophys. Res.*, **99**, 5551–5568.
- Hao, W. M., and M.-H. Liu, 1994: Spatial and temporal distribution of tropical biomass burning. *Global Biogeochemical Cycles*, **8**, 495–503.
- Holtlag, A., and B. Boville, 1993: Local versus nonlocal boundary-layer diffusion in a global climate model. *J. Climate*, **6**, 1825–1842.
- Horowitz, L. W., and Coauthors, 2003: A global simulation of tropospheric ozone and related tracers: Description and evaluation of MOZART, version 2. *J. Geophys. Res.*, **108**(D24), 4784, doi:10.1029/2002JD002853.
- IPCC, 2001: *Climate Change 2001: The Scientific Basis*. Contribution of Working Group 1 to the Third Assessment Report of the Intergovernmental Panel on Climate Change, J. T. Houghton et al., Eds., Cambridge University Press, Cambridge, 881pp.
- Kiehl, J. T., J. J. Hack, G. B. Bonan, B. A. Boville, D. L. Williamson, and P. J. Rasch, 1998: The National Center for Atmospheric Research Community Climate Model: CCM3. *J. Climate*, **11**, 1131–1149.
- Lin, S.-J., and R. B. Rood, 1996: Multidimensional flux-form semi-Lagrangian transport schemes. *Mon. Wea. Rev.*, **124**, 2046–2070.
- Liu Yu, I. S. A. Isaksen, J. K. Sundet, Zhou Xiuji, and Ma Jianzhong, 2003: Impact of aircraft NO<sub>x</sub> emission on NO<sub>x</sub> and ozone over China. *Adv. Atmos. Sci.*, **20**(4), 565–574.
- Liu Yu, I. S. A. Isaksen, J. K. Sundet, and He Jinhai, 2004: NO<sub>x</sub> changes over China and its influences. *Adv. Atmos. Sci.*, **21**(1), 132–140.
- Logan, J. A., 1985: Tropospheric ozone: Seasonal behavior, trends and anthropogenic influence. *J. Geophys. Res.*, **90**, 10463–10482.
- Logan, J. A., 1999: An analysis of ozonesonde data for the troposphere: Recommendations for testing 3-D models and development of a gridded climatology for tropospheric ozone. *J. Geophys. Res.*, **104**, 16115–16149.
- Maxobep, M., 1983: *Tropopause Meteorology*. Translated by Zhang Guiyen and Liao Shoufa, China Meteorological Press, Beijing, 283pp. (in Chinese)
- Monks, P. S., G. Holland, G. Salisbury, S.A. Penkett, and G.P. Ayers, 2000: A seasonal comparison of ozone photochemistry in the remote marine boundary layer. *Atmos. Environ.*, **34**, 2547–2561.

- Müller, J.-F., 1992: Geographical distribution and seasonal variation of surface emissions and deposition velocities of atmospheric trace gases. *J. Geophys. Res.*, **97**, 3787–3804.
- Olivier, J. G. J., and Coauthors, 1996: Description of EDGAR version 2.0: A set of global emission inventories of greenhouse gases and ozone-depleting substances for all anthropogenic and most natural sources on a per country basis and on a  $1 \times 1$  degree grid, RIVM Rep. 771060 002/TNO-MEP Rep. R96/119, Natl. Inst. of Public Health and Environ., Bilthoven, Netherlands, 141pp.
- Randel, W. J., F. Wu, J. M. Russell III, A. Roche, and J. Waters, 1998: Seasonal cycles and QBO variations in stratospheric  $\text{CH}_4$  and  $\text{H}_2\text{O}$  observed in UARS HALOE data. *J. Atmos. Sci.*, **55**, 163–185.
- Rasch, P. J., N. W. Mahowald, and B. E. Eaton, 1997: Representations of transport, convection, and the hydrologic cycle in chemical transport models: Implications for the modeling of short-lived and soluble species. *J. Geophys. Res.*, **102**, 28127–28138.
- SASAKI G., 2003: Atmospheric CO and O<sub>3</sub> daily mean measurements at both Minamitorishima and Ryori, <http://gaw.kishou.go.jp/wdcgg.html>, World Data Cent. for Greenhouse Gases, Tokyo.
- Zhang, G. J., and N. A. McFarlane, 1995: Sensitivity of climate simulations to the parameterization of cumulus convection in the Canadian Climate Centre General Circulation Model. *Atmos. Ocean*, **33**, 407–446.
- Zhang Meigen, Xu Yongfu, Itsushi UNO, and H. Akimoto, 2004: A numerical study of tropospheric ozone in spring in East Asia. *Adv. Atmos. Sci.*, **21**(2), 163–170.